

# Characterization of Damped Structural Connections for Multi-Component Systems

Charles Lawrence  
*Lewis Research Center*  
*Cleveland, Ohio*

and

Arthur A. Huckelbridge  
*Case Western Reserve University*  
*Cleveland, Ohio*

(NASA-TM-100801) CHARACTERIZATION OF DAMPED  
STRUCTURAL CONNECTIONS FOR MULTI-COMPONENT  
SYSTEMS (NASA) 19 p CSCL 20K

88-18974

Unclassified  
G3/39 0130089

March 1988



CHARACTERIZATION OF DAMPED STRUCTURAL CONNECTIONS  
FOR MULTI-COMPONENT SYSTEMS

Charles Lawrence  
National Aeronautics and Space Administration  
Lewis Research Center  
Cleveland, Ohio 44135

and

Arthur A. Huckelbridge  
Case Western Reserve University  
Cleveland, Ohio 44106

SUMMARY

The inability to model connections adequately has historically limited the ability to predict overall system dynamic response. Connections between structural components are often mechanically complex and difficult to accurately model analytically. Improved analytical models for connections are needed to improve system dynamic predictions. This study explores combining Component Mode Synthesis methods for coupling structural components with Parameter Identification procedures for improving the analytical modeling of the connections. Improvements in the connection stiffness and damping properties are computed in terms of physical parameters so the physical characteristics of the connections can be better understood, in addition to providing improved input for the system model.

E-3980

INTRODUCTION

Analytical models of structural systems normally do not normally possess characteristics which agree completely with those obtained from experiments. Although there are many possible explanations for the discrepancies, the major causes often can be attributed to inaccuracies in the data used to create the analytical model. Parameters such as material and dimensional properties, which are usually obtained from nominal design specifications, can differ considerably from the true values, thus causing the analytical model to be inaccurate. Structural properties such as damping and connection stiffnesses also are extremely difficult to predetermine, yet their influence on structural response predictions is profound.

For large structural systems it is common practice to utilize substructuring methods to create the analytical system model. These methods are used to construct the model by partitioning the structure into components, and then linking the individual components together with inter-component connections. The components frequently can be modeled with reasonable accuracy whereas the connections are difficult, or in many situations impossible to analytically model. This is especially true when the connections contain significant amounts of damping.

The objective of the present work is to investigate the feasibility of determining the characteristics of viscously damped connections from test data obtained from the complete coupled system. It is desirable to be able to determine the connection stiffness and damping from tests performed on the complete system so that the difficulties associated with testing individual joints can be circumvented. The problem with testing individual joints is that often special test fixtures are required for mounting the joint. Also, conventional modal tests can not be performed on the joint because joints normally are very stiff, and thus require static and cyclic loading tests in determining stiffness and damping properties (ref. 1). Furthermore, although several joints may be nominally identical, their actual properties may vary enough to require that every joint be tested. When system tests are performed the difficulties associated with tests on individual joints are eliminated. Instead of special fixtures the system can be tested in its actual operating environment or hung from flexible suspenders. Conventional modal tests which are much simpler to perform than static or cyclic loading tests can generally be used because the system modes are in a suitable range. Also, the low frequency modal data contains information about the joints even though the joints themselves are relatively stiff.

Several previous studies have addressed the issue of identifying the stiffness of connections without considering damping. In reference 2 an attempt was made to identify the stiffness of connections by using a combination of a weighted least squares parameter identification and substructuring methods. This work showed that physical stiffness characteristics can be determined from experimentally obtained frequency data as long as sufficient test data are available. In reference 3 the stiffness characteristics of the connections between the Centaur G Prime Launch Vehicle and the shuttle orbiter were modified based on experimentally obtained modal data. The connections were altered so that a test-verified analytical model would be available for subsequent loads analysis. The modifications, based on engineering intuition and judgement were deemed satisfactory when the analytical and experimental frequency data were in agreement.

Previous studies that have addressed connection damping (refs. 1, and 4 to 8) have focused on identifying damping properties from tests on individual joints rather than from coupled system tests. In reference 1 a mix of analytical and experimental component models were combined to characterize the dynamics of a flexible spacecraft. For this study, joint stiffness and damping were ascertained before the joints were incorporated into the system model. Data obtained from cyclic loading tests indicated that the joint damping was primarily viscoelastic, although it was noted that joints in actual space structures may exhibit nonlinearities and friction damping. Since the system modal properties computed from the experimentally derived joint models were in agreement with test results, there was no need to modify the joint characteristics by using the coupled system test data. In reference 4 damping and stiffness characteristics of a representative space truss joint were studied. In that work results from simplified joint models were compared to results obtained from a complex model which included dead bands, large deformations, and friction forces. It was concluded that simplified models based on linear springs and viscous dampers could represent the behavior of the more sophisticated joint model. No actual experimental data was used in that study. In reference 5 nonlinearities in a structural joint were identified by using an approach termed "force-state mapping". This approach involved simultaneously measuring the force on a joint along with its position and velocity. From the

shape of the three dimensional surface generated by plotting force as a function of displacement and velocity the type and quantitative description of the joint mechanisms were identified.

In the present paper a general procedure for component coupling is presented. This procedure accommodates components that have been modeled with either, finite elements or with modal data which has been obtained from analytical models or experiment. A parameter identification procedure based on the weighted least squares method also is introduced. This procedure utilizes system test data to find an optimal set of stiffness and viscous damping connection properties. Finally, two example problems using simulated experimental data are presented. For these problems both stiffness and damping connection properties are identified. A Monte-Carlo simulation is run to assess the effect of variance in the experimental data on the identified properties in the first problem. The effect of friction damping is evaluated in the second.

### COMPONENT COUPLING PROCEDURE

The approach used for developing the coupled system equations of motion is extrapolated from the procedure of reference 9. In this approach component models are represented through the use of finite elements or with modal data. Component modal data may be obtained from experiment, or from a reduced finite element model. Once the component models are obtained, they are coupled at physical boundary degrees of freedom through physical connecting elements. In the present work both stiffness and viscous damping is accommodated in the connecting elements. Residual flexibility, which is discussed in reference 9 also is included.

Consider the system shown in figure 1. This system is comprised of two components which are coupled by a single connecting element. The damped equation of motion for the uncoupled system is written as:

$$\begin{bmatrix} [M^I] & & \\ & [0] & \\ & & [M^{II}] \end{bmatrix} \begin{Bmatrix} \ddot{U}^I \\ \ddot{X}^C \\ \ddot{U}^{II} \end{Bmatrix} + \begin{bmatrix} [0] & & \\ & [C^C] & \\ & & [0] \end{bmatrix} \begin{Bmatrix} \dot{U}^I \\ \dot{X}^C \\ \dot{U}^{II} \end{Bmatrix} + \begin{bmatrix} [K^I] & & \\ & [K^C] & \\ & & [K^{II}] \end{bmatrix} \begin{Bmatrix} U^I \\ X^C \\ U^{II} \end{Bmatrix} = \{0\} \quad (1)$$

where  $[M]$ ,  $[C]$ , and  $[K]$  are the system mass, damping, and stiffness matrices respectively,  $\{\ddot{u}\}$ ,  $\{\dot{u}\}$ , and  $\{u\}$  are the corresponding accelerations, velocities, and displacements in terms of physical and/or modal coordinates, and  $\{\ddot{x}\}$ ,  $\{\dot{x}\}$ , and  $\{x\}$  are the physical accelerations, velocities, and displacements at the connections. (Superscripts refer to component identifications.) Note that the connecting component is massless, and the other two components have no damping. For many systems it is reasonable to assume that the actual component damping is negligible, and that any significant damping is isolated in the connections.

Once partitioning between boundary and internal degrees of freedom has been completed, and displacement compatibility between components has been implemented, the coupled system equations of motion for the damped system may be derived as follows:

$$\begin{bmatrix} M^I \\ & M_{bb}^I \end{bmatrix} \begin{bmatrix} \ddot{U}_1^I \\ \ddot{X}_b^I \end{bmatrix} + \begin{bmatrix} 0 & C^c \\ -C_{II\ I}^c & 0 \end{bmatrix} \begin{bmatrix} \dot{U}_1^I \\ \dot{X}_b^I \end{bmatrix} + \begin{bmatrix} K^I & -K_{Ib}^I \\ -K_{Ib}^{I\ T} & K_{bb}^I + K_I^c \end{bmatrix} \begin{bmatrix} U_1^I \\ X_b^I \end{bmatrix} = \{0\} \quad (2)$$

$$\begin{bmatrix} M_{bb}^{II} \\ & M^{III} \end{bmatrix} \begin{bmatrix} \ddot{U}_1^{II} \\ \ddot{X}_b^{II} \end{bmatrix} + \begin{bmatrix} C_{II\ I}^c & 0 \\ C_{II\ I}^c & 0 \end{bmatrix} \begin{bmatrix} \dot{U}_1^{II} \\ \dot{X}_b^{II} \end{bmatrix} + \begin{bmatrix} -K_{II\ I}^c & K_{bb}^{II} + K_{II}^c \\ -K_{II\ I}^{c\ T} & -K_{IIb}^{II} \end{bmatrix} \begin{bmatrix} U_1^{II} \\ X_b^{II} \end{bmatrix} = \{0\}$$

where the component degrees of freedom  $\{u\}$  are partitioned into internal  $\{u_i\}$  and physical boundary  $\{x_b\}$  degrees of freedom. For components modeled with finite elements, all of the degrees of freedom are physical. For modal components, the boundary degrees of freedom are physical while the internal,  $\{u_i\}$ , degrees of freedom are represented in terms of modal coordinates.

When modal data is used to characterize components, physical degrees of freedom at the component boundary must be derived from the modal data before the component can be input into equation (2). These degrees of freedom are obtained by transforming a subset of the modal coordinates into physical coordinates. The equation of motion for an undamped modal component including the diagonal terms of the residual flexibility matrix associated with the boundary degrees of freedom is:

$$\begin{bmatrix} M^* \\ & q_b \end{bmatrix} \begin{bmatrix} \ddot{q}_k \\ .. \end{bmatrix} + \begin{bmatrix} K^* \\ & q_b \end{bmatrix} \begin{bmatrix} q_k \\ q_b \end{bmatrix} = \{0\} \quad (3)$$

$$[M^*] = \begin{bmatrix} I_{kk} & 0 \\ 0 & 0 \end{bmatrix} \quad [K^*] = \begin{bmatrix} w_{kk}^2 & 0 \\ 0 & G_{bb}^d \end{bmatrix}$$

where  $\{q\}$  are modal coordinates,  $[I_{kk}]$  is the identity matrix,  $[w_{kk}^2]$  is the matrix of component frequencies, and  $k$  is the number of measured or retained modes.  $[G_{bb}^d]$  is the diagonal matrix of residual flexibilities,

$$\sum_{j=k+1}^N \frac{\phi_{jb} \phi_{jb}^T}{w_j^2} \text{ at the boundary, } b, \text{ degrees of freedom.}$$

The matrix  $G_{bb}^d$ , containing the component residual flexibility is computed by summing all of the missing modal data  $(k+1, N)$  at each of the boundary degrees of freedom. Experimentally, the entries in the residual flexibility matrix are obtained by determining the differences between the curve fit and the experimentally measured frequency response functions (ref. 10). The residual flexibility is implemented so that flexibility which is not contained in the truncated set of component modes is included in the component model. The values of the residual flexibilities at the boundary are required because they provide information necessary for accurate component coupling and for the creation of a precise system model. Only the diagonal terms in the matrix are used here because it has been found that the off-diagonal terms, which relate the cross coupling between boundary degrees of freedom, have a negligible effect on the fidelity of the model (ref. 9).

Using the transformation:

$$\begin{pmatrix} x_i \\ x_b \end{pmatrix} = \begin{bmatrix} \phi_{ik} & 0 \\ \phi_{bk} & G_{bb}^d \end{bmatrix} \begin{pmatrix} q_k \\ q_b \end{pmatrix} \quad (4a)$$

leads to:

$$\begin{pmatrix} q_k \\ q_b \end{pmatrix} = \begin{bmatrix} I & 0 \\ -G^{-1}\phi_{bk} & G^{-1} \end{bmatrix} \begin{pmatrix} q_k \\ x_b \end{pmatrix} \quad (4b)$$

Using the above transformation and equation 3, the component equations of motion in terms of modal and physical boundary coordinates are derived as:

$$\begin{bmatrix} I & 0 \\ 0 & I \end{bmatrix} \begin{pmatrix} \ddot{q}_k \\ x_b \end{pmatrix} + \begin{bmatrix} W_{kk}^2 + \phi_{bk}^T G^{-1} \phi_{bk} & -\phi^T G^{-1} \\ -G^{-1} \phi_{bk} & G^{-1} \end{bmatrix} \begin{pmatrix} q_k \\ x_b \end{pmatrix} = \{0\} \quad (5)$$

After the component equations are transformed into the coordinate system used in equation (5), the component can then be incorporated into the system equations in the same manner as are the finite element components.

Once the system equations of motion are constructed, they can be used to predict the system frequencies and mode shapes. This modal data is then used in conjunction with the experimentally measured modal parameters to identify the connection properties. Because the system is damped, the frequencies will be complex; the real part corresponding to the modal damping and the imaginary part to the modal frequency. The mode shapes also will be complex but for most damped systems (including the present research) the imaginary part can be disregarded.

#### PARAMETER IDENTIFICATION PROCEDURE

Several methods are available for parameter identification (ref. 11). The methods which incorporate optimization strategies can be classified into three groups; least squares, weighted least squares, and Bayesian estimation. With the least squares method the set of parameters which minimizes the difference between the measured and predicted response is computed. The weighted least squares method is similar except that a "weight," corresponding to the relative confidence in the measured data, is incorporated. The Bayesian method permits specification of the randomness of the parameters that are being computed as well as the confidence in the measured data. Since in practice the randomness of the connection parameters may be difficult to quantify the Bayesian method normally is not useful. The weighted least squares method will be used in the present study because it is feasible and useful to quantify the confidence levels in the measured data.

Assuming that the component characterizations are accurate, and that an appropriate set of component modes has been used to represent the overall system response, a search can be initiated for a set of connection parameters

which better predicts the system frequencies and mode shapes. The assumption that the component representation is accurate may require that experimental verification be performed on the component models before they are used in the system characterization. Although this approach may require additional effort in that verified component models are required, it greatly simplifies the parameter identification by limiting the location of possible inaccuracies to the connections. The requirement that an appropriate set of component modes be used normally can be met by including the lower modes, and by utilizing a number of degrees of freedom in the system model that is at least twice the number of modes of interest (a mode equates to 1° of freedom). This requirement is comparable to the modeling guidelines used for conventional finite elements. By including residual flexibilities, the requirement can be relaxed.

The parameter identification (PID) discussed in reference 2 is used here to find an improved set of connection parameters that better predict the measured system data. The difference between this work and the work in reference 2 is that in this work modal damping is included in the identification.

The improved set of connection parameters are computed iteratively from:

$$\{r\} = \{r\}_{EST} + ([S]^T[W][S])^{-1}[S]^T[W](\{\bar{c}\} - \{c\}_{EST}) \quad (6)$$

where  $\{r\}$  is the vector of improved connection parameters (physical stiffness and damping coefficients),  $\{c\}_{MES}$  and  $\{c\}_{EST}$  are the measured and computed system modal parameters,  $[W]$  is a weighting matrix for the measured data, and  $[S]$  is a sensitivity matrix containing the partial derivatives,  $d\{c\}/d\{r\}$ .

The vector of measurements,  $\{c\}$ , can contain both complex frequency (frequency and damping), and/or mode shape data. For the mode shape data it is sensible to use a measure of the overall fit between the predicted and experimental mode shape instead of using values of the mode shapes at individual locations. A logical measure of the overall fit is the least squares difference between mode shape data points. The Mode Shape Correlation Coefficient (ref. 12) provides this kind of measure. The Mode Shape Correlation Coefficient is advantageous because it provides a quantitative measure of the fit between the entire analytical and experimental mode shape, and furthermore, it does not require the experimental and computed mode shapes to be normalized in the same manner.

The weighting matrix,  $[W]$ , is used for specifying the confidence levels as well as for scaling the system modal parameters. For example, to specify that the modal damping has equal importance to the frequency, a larger weight may need to be placed on the damping parameter. This is due to the fact that the order of magnitude of modal damping is less than that of frequency. Also, a higher weight may be warranted for parameters that are more significant, or that have been measured with greater accuracy.

The sensitivity matrix,  $[S]$ , although relatively laborious, is straightforward to compute. In the present study the sensitivity matrix is computed by perturbing the system with small changes in the connection parameters,  $\{r\}$ , and then recording the resulting changes in the system modal parameters,  $\{c\}_{EST}$ . A new sensitivity matrix is computed for each iteration of equation (6).

## SAMPLE PROBLEM ONE

The first sample problem is presented to demonstrate the parameter identification procedures and to assess the feasibility of identifying physical connection properties from coupled system modal data. For this problem a finite element model was used to generate simulated experimental data. The model (fig. 2) consists of three planar elastic beams connected at their ends with revolute (pinned) connections. Each connection is attached to ground by a linear, translational, spring, and viscous damper. The properties of the connections are varied by changing the value of 'm' and 'n' which are shown in the figure. Each of the beam components is discretized into five beam elements with the beam mass lumped at the ends of the elements. The complex eigenvalue extraction capabilities (Sol 28) of MSC NASTRAN (ref. 13) were used to compute the simulated experimental frequencies, modal damping, and mode shapes for the coupled system. NASTRAN also was used for computing the free-free modes for the individual beam components. These modes are used for creating the modal components for the analytical model. Four modes, two rigid body and two elastic, were used for the component representations.

Figure 3 shows the effect that the grounded springs have on the system's undamped resonant frequencies. The results in this figure are generated from the experimental model. For  $n = 0$ , the first four modes resemble rigid body modes, reflecting the softness of the springs. As ' $n$ ' is increased the system becomes stiffer, the frequencies increase, and the system behaves more like a series of simply supported beams. For ' $n$ ' greater than eight, the grounded springs act as rigid supports. In the subsequent parameter identification, a range of ' $n$ ' values is investigated so that a performance assessment can be made for both very flexible, and relatively rigid, connections.

In figure 4, a comparison is made between resonant frequencies from the modal model (residual flexibilities not included) and those from the experimental model. Since four modes were used to represent each component, and there are three components, the system modal model had twelve degrees of freedom. Based on this number of degrees of freedom it was expected that the first four or five modes could be predicted with reasonable accuracy. For low ' $n$ ' values there is very good agreement between the experimental and component mode models for the first five modes. This is expected since the component mode model is generated from free-free component modes. For low ' $n$ ', each component behaves as if it were freely supported. For larger ' $n$ ' values the system behaves like a series of simply supported beams, creating greater disagreement between the frequencies predicted by the experimental and modal models. This also is expected because the truncated component mode representation is better suited for predicting rigid body type motions, and has a more difficult time with the bending type behavior of the simply supported components. The mismatch for high ' $n$ ' values is still moderate, especially for the first three system resonant frequencies. Obviously, when more or less than four component modes are used the respective mismatch decreases and increases. In general, the modal model utilizing four component modes produced very reasonable results. When residual flexibility was included there almost was perfect agreement over the entire range of ' $n$ ' values.

In figure 5, the differences between the experimental and identified connection stiffnesses are plotted as a function of ' $n$ ' value. The connection

values were identified by minimizing the differences between the first seven system resonant frequencies. Mode shape data was not utilized. It was preferable not to have to use any mode shape data because shape data is considerably more difficult to measure experimentally than are frequencies. To initiate the parameter identification (eq. (6)), initial estimates are required for the connection parameters. In creating the data shown in this figure, zero stiffness values were used for the initial estimates of the connection parameters. When the connection properties are better known, the initial estimates can be improved, and convergence is accelerated.

The strongest agreement between experiment and computed connection parameters is at ' $n$ ' = 4. This is in contrast to the highest frequency match (fig. 4) which was at ' $n$ ' = 0. Even at ' $n$ ' = 0, where the difference is as large as thirty percent, the match is still fairly good considering the prevalent difficulties associated with determining connection properties. In many situations it is adequate merely to be able to determine the order of magnitude of the connection properties. For ' $n$ ' = 6, converged parameters could not be computed without including residual flexibilities, although the order of magnitude of the connection properties was determined correctly. With the inclusion of residuals, the connection stiffnesses were computed to within forty percent accuracy.

There are two reasons why disparities between the identified and experimental connection values may occur, even though the analytical model accurately predicts the system frequencies (e.g., at ' $n$ ' = 0,2,4). The first reason is that when the frequencies are relatively insensitive to the connection stiffnesses, a high degree of precision in the experimental data is required for accurate identification. In practice, this required degree of precision may not be attainable and only an order of magnitude estimate of the connection properties may be realized. The second explanation involves the existence of multiple solutions. For many systems, including the one presented in this paper, more than one set of connection properties exists which satisfies the objective of eliminating the differences between the measured and predicted modal parameters. When this is the case, the resulting set of connection properties is dependent on the initial estimates for the connections and on the step size used for computing the sensitivity matrix. Normally, the number of solutions can be minimized by utilizing additional frequencies and/or mode shapes in the identification. The number of possible solutions and the required quantity of experimental data can be determined beforehand by performing simulation studies with varying step sizes and initial estimates for the connection properties.

The data in figures 6(a) and (b) were created to assess the effect of damping on the identification of connection properties. For these figures, the connection stiffnesses were held constant at ' $n$ ' = 4, and the damping was varied from ' $m$ ' = 0 to 1.4 (critical damping is near ' $m$ ' = 1.6). In figure 6(a) the flatness of the curves demonstrate the insensitivity of the stiffness computations to damping. Even for large damping, ' $m$ ' = 1.4, the connection stiffnesses are computed accurately. In figure 6(b) the effect of damping on the identified connection damping is displayed. Similar to the stiffness results, the identified damping also is fairly insensitive to the level of the damping. In general, when the level of damping is low, and hence frequency is unaffected by damping, there will not be any coupling between damping and stiffness, and the connection stiffness and damping properties may be identified independently.

A Monte Carlo simulation was used to assess the accuracy of the parameter identification for various degrees of experimental error. Normally, the level of experimental error in frequency is small, while the error in damping and mode shapes is relatively large. Based on this assumption, the coefficient of variation in the frequency measurements was set at 1 percent and the damping coefficient of variation was varied from 1 to 15 percent. For simplicity, mode shape data was not utilized. Simulated data was generated by making forty runs at ' $n$ ' = 4, ' $m$ ' = 1.2, and using a random number generator to select the experimental modal frequencies and damping (normal distributions were assumed). Plots displaying the probability of achieving a precision level for the various degrees of measurement coefficient of variation are shown in figures 7(a) and (b). In these figures it is shown that as the coefficient of variation in the measured data increases, the probability of achieving a given level of precision decreases. For example, the probability of identifying the damping to within 20 percent of the actual damping is nearly 80 percent for a damping coefficient of variation of 1 percent, while it is less than 40 percent for a coefficient of variation of 15 percent. Obviously, as the required precision level is relaxed, the probability of reaching that level is increased.

From figure 7(b) it is evident that regardless of the damping coefficient of variation, the identified stiffness properties are reasonably precise. For example, the probability of attaining a 30 percent precision is very good (greater than 80 percent) for all three levels of damping coefficient of variation. These results were expected since for the mean damping used for the simulation (' $m$ ' = 1.2) the stiffness is fairly independent of damping. It should be noted that the results from the Monte Carlo simulation are problem dependent and can only be used for providing insight into the degree of accuracy that might be expected for other problems.

## SAMPLE PROBLEM TWO

The connections in many structural systems contain nonlinearities such as friction or gaps. For multi-degree of freedom systems it is virtually impossible to identify and characterize all of the complexities that may exist in connections. Often, a simplifying assumption is made that the connection damping can be adequately described by linear viscous dampers even though other types of damping exist in the connection. With this assumption the identification process and subsequent analysis are greatly simplified. In the second sample problem the effects of the viscous damping assumption are assessed by adding friction damping into the system. First, the effect of friction damping on the identified viscous damping connection properties is determined. Subsequently, a comparison is made between the actual response of the system with friction damping and the response of the identified system with the friction damping approximated by viscous damping.

The structure utilized for the second sample problem is identical to the first except that friction dampers have been added at each of the connection locations (fig. 8). The friction dampers at each of the four connections were identical. The viscous dampers and grounded springs which were used in the first sample problem also were used here. The parameters for these elements (see fig. 2) were fixed at  $m = 1$  and  $n = 4$ .

MSC/NASTRAN Solution 99 was used to compute the modal damping for the coupled system. The damping was computed by exciting the system and then allowing it to decay (fig. 9). The rate of free decay then was used to compute an equivalent modal damping for each of the first seven modes at different levels of friction damping. To obtain the free decay response each mode was individually excited by applying a distributed sinusoidal load at the modal frequency with the same distribution as the mode shape. The magnitude of the sinusoidal load was set so that the resulting displacements were on the order of the system span/100. The excitation frequency and distribution was determined by assuming that the modal frequencies and mode shapes would be unchanged from the system without friction damping.

Equivalent viscous damping ratios were computed for four levels of friction damping. The friction ratio was defined as the ratio of the friction force at each of the four connection locations to the maximum value of the distributed sinusoidal excitation. Damping ratios were computed at friction ratios of  $r = 0.0$ ,  $r = 0.02$ ,  $r = 0.10$ , and  $r = 0.50$ . The resulting modal damping values are given in table I. As expected, the equivalent modal damping increases with an increase in friction force. The damping ratios from this table next were used in the parameter identification to compute equivalent viscous dampers. The identified viscous dampers are given in table II. Without friction damping,  $r = 0.00$ , the identified dampers are very close in value to the actual dampers. When friction is present, the identified dampers do not appear to follow any pattern, but they do enable the predicted frequencies and modal damping to match the experimental data closely.

The performance of the identified models was assessed by comparing transient responses of the identified models to those from the experimental models at each of the four levels of friction damping. The models were excited by applying a step function input load at the center of the system. The effect of the step input is to excite all of the system modes, with a greater emphasis on the lower modes. The resulting system response, shown in figure 10, reaches a peak displacement just after the step load is applied and then decays while oscillating about a steady state displacement. The responses from the identified and experimental models were evaluated by comparing peak response, settling time, and RMS error (see table III). At all four friction levels there was very little error in peak response (e.g., only 2 percent error at  $r = 0.50$ ). The settling time error, which is defined as the error in time to reach 10 percent of the steady state displacement, increased considerably from the lower to higher levels of friction damping. For example, at  $r = 0.50$  the time it took for the identified model to reach steady state displacement was twice that of the experimental model (122 percent error).

The Fourier transforms of the displacement responses were computed for  $r = 0.10$  and  $r = 0.50$  (figs. 11(a) and (b)). To clarify these transforms, the steady state displacements were subtracted from the displacement responses. From the Fourier transforms it is seen that most of the discrepancy between the experimental and identified model responses can be attributed to the difference in contribution of the first mode. For both  $r = 0.10$  and  $r = 0.50$  transforms there is minimal difference, except for the first mode where the difference is extreme.

In figure 12, the amplitude and settling time errors are compared at three magnitudes of input load while the friction force was held constant at  $r = 0.10$ . Since the friction damping is amplitude dependent (inversely proportional to displacement and frequency), it was expected that the identified model would accurately match the experimental model response only at the same excitation levels and distributions as were used to compute the equivalent viscous damping ratios. Considering that the equivalent viscous dampers were derived by using sinusoidal excitation, and the responses in the figure are the result of a step input excitation, the identified model does a fairly reasonable job of predicting the experimental response for a broad range of excitation levels and distributions. As expected, the identified model over-estimates the system damping at high amplitudes. This is because the equivalent viscous damping is inversely proportional to amplitude and therefore would have to be decreased for higher amplitude response.

#### SUMMARY AND CONCLUSIONS

A method for coupling multi-component systems, and for identifying connection stiffness and damping characteristics was developed and verified with simulated data. In the first sample problem component connection properties were determined for a three component planar beam model. From this analysis it was found that properties could be accurately identified for a broad range of connection stiffnesses and damping using relatively minimal measured data. The connection properties were identified using frequency data alone. Mode shape data was not required. By performing a Monte-Carlo simulation it was determined that connection damping and stiffness can be identified even in the presence of experimental error.

In the second sample problem equivalent viscous connection damping was identified for a model actually having friction and viscous damping. A comparison between the experimental and identified model showed that for particular ranges of input excitation the identified model could reliably predict peak response and settling time. However, at high levels of friction damping, the identified model did not perform as well. Since many systems include connections with nonlinearities, it is important that unrealistic predictions concerning the in-service response of the system are not made. Instead, the extent of any nonlinearity should be determined by inspection of the measured data, and then the subsequent effect of any identified nonlinearity on system response should be explored.

#### REFERENCES

1. Soni, M.L.; and Agrawal, B.N.: Damping Snythesis for Flexible Space Structures Using Combined Experimental and Analytical Models. AIAA Paper 85-0779, Apr. 1985.
2. Huckelbridge, A.A.; and Lawrence, C.: Identification of Structural Interface Characteristics Using Component Mode Snythesis. NASA TM-88960, 1987.
3. Chen, J., et al.: Modal Test/Analysis Correlation for Centaur G Prime Launch Vehicle. AIAA Paper 86-1002, May 1986.

4. Ferri, A.A.: Investigation of Damping From Nonlinear Sleeve Joints of Large Space Structures. Role of Damping in Vibration and Noise Control, L. Rogers and J.C. Simonis, eds., ASME, 1987, pp. 187-195.
5. Crawley, E.F.; and Aubert, A.C.: Identification of Nonlinear Structural Elements by Force-State Mapping. AIAA J., vol. 24, no. 1, Jan. 1986, pp. 155-162.
6. Hertz, T.J.; and Crawley, E.F.: Damping in Space Structure Joints. AIAA Paper 84-1039, May 1984.
7. Bohlen, S.; and Gaul, L.: Vibrations of Structures Coupled by Nonlinear Transfer Behaviour of Joints; A Combined Computational and Experimental Approach. Proceedings of the 5th International Modal Analysis Conference, Union College, Schenectady, NY, 1987, pp. 86-91.
8. Hertz, T.J.; and Crawley, E.F.: Displacement Dependent Friction In Space Structural Joints. AIAA J., vol. 23, no. 12, Dec. 1985, pp. 1998-2000.
9. Martinez, D.R.; and Gregory, D.L.: A Comparison of Free Component Mode Synthesis Techniques Using MSC/NASTRAN. SAND-83-0025, June 1984.
10. Lamontia, M.A.: On the Determination and Use of Residual Flexibilities, Inertia Restraints, and Rigid-Body Modes. Proceedings of the First International Modal Analysis Conference and Exhibit, Union College, Schenectady, NY, 1982, pp. 153-159.
11. Isenberg, J.: Progressing From Least Squares to Bayesian Estimation. ASME Paper 79-WA/DSC-16, Dec. 1979.
12. Ewins, D.J.: Modal Testing: Theory and Practice. Research Studies Press, 1984.
13. MSC/NASTRAN Users Manual, MacNeil-Schwendler Corp., 1981.

TABLE I. - EQUIVALENT VISCOS DAMPING RATIOS,  $\epsilon$ 

Mode	$r = 0$	$r = 0.02$	$r = 0.10$	$r = 0.50$
94.9 Hz	0.024	0.031	0.048	0.082
119	.027	.035	.051	.100
145	.031	.032	.042	.080
208	.040	.036	.045	.110
307	.040	.041	.054	.100
408	.032	.035	.037	.080
484	.060	.063	.067	.140

TABLE II. - IDENTIFIED EQUIVALENT VISCOS DAMPERS

	$C_1$	$C_2$	$C_3$	$C_4$
$r = 0.00^a$	9.4	21	27	37
$r = 0.02$	20.6	7.7	23.3	43.6
$r = 0.10$	26.2	7.7	45.3	34.6
$r = 0.50$	25.1	52	54	53

<sup>a</sup>Actual values are  $C_1 = 10$ ,  $C_2 = 20$ ,  $C_3 = 30$ , and  $C_4 = 40$ .

TABLE III. - EVALUATION OF IDENTIFIED MODELS

	Peak amplitude (experimental)	Peak amplitude error, percent	Settling* time error, percent	RMS error
$r = 0.00$	0.755	0	0	0.00
$r = 0.02$	.754	2	13	.07
$r = 0.10$	.750	3	44	.11
$r = 0.50$	.731	2	122	.24

\*Settling time = time to reach  $\pm 10$  percent of steady state displacement.

U = PHYSICAL AND/OR MODAL DEGREES OF FREEDOM  
X = PHYSICAL DEGREES OF FREEDOM

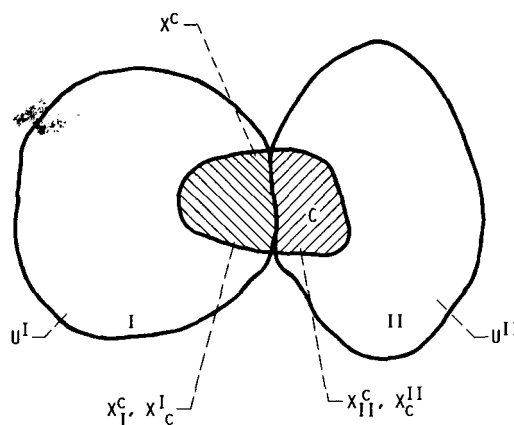


FIGURE 1. - THREE COMPONENT SYSTEM.

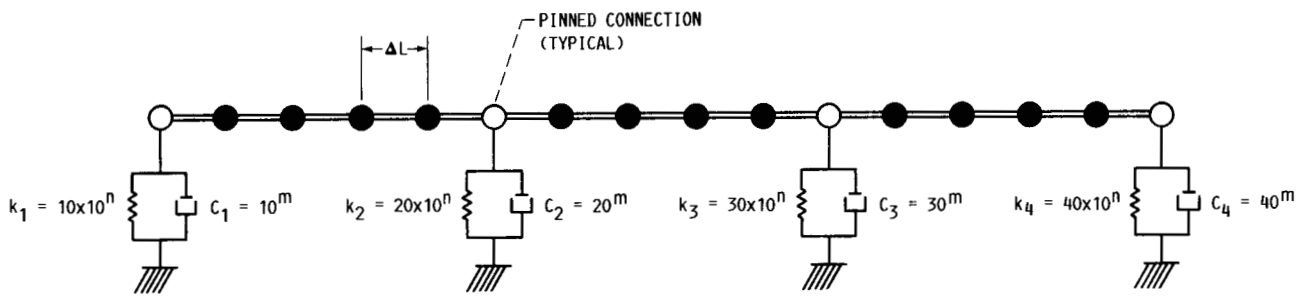


FIGURE 2. - THREE COMPONENT COUPLED SYSTEM ( $EI = 10^5$ ,  $\rho = 0.10$ ,  $\Delta L = 1.0$ ).

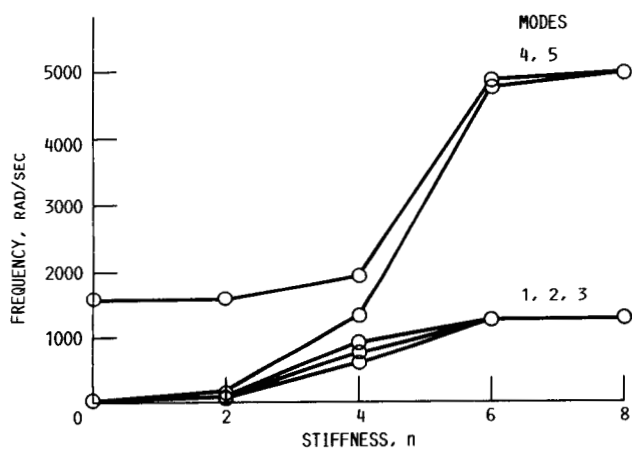


FIGURE 3. - MODAL FREQUENCIES FOR UNDAMPED EXPERIMENTAL MODEL.

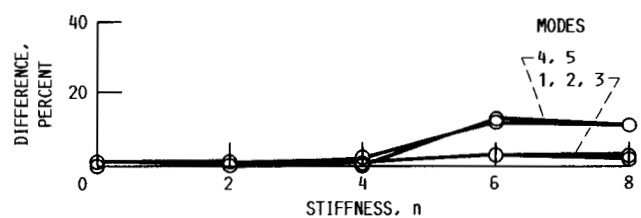


FIGURE 4. - FREQUENCY DIFFERENCE BETWEEN MODAL AND EXPERIMENTAL MODEL.

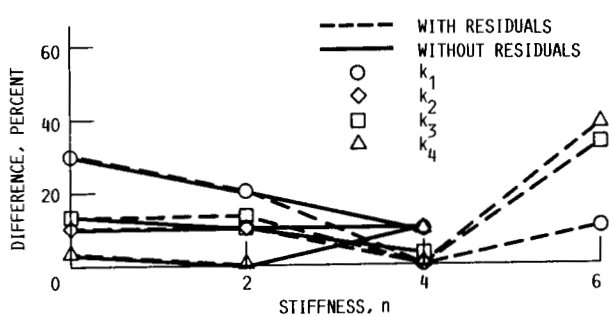


FIGURE 5. - DIFFERENCES BETWEEN IDENTIFIED AND EXPERIMENTAL CONNECTION STIFFNESSES (UNDAMPED).

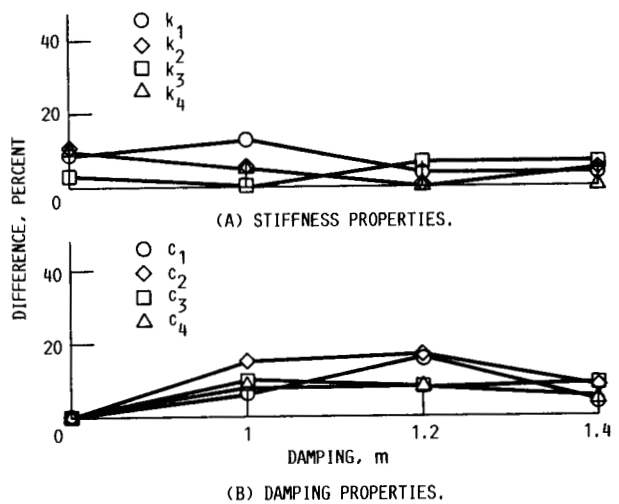


FIGURE 6. - DIFFERENCES BETWEEN IDENTIFIED AND EXPERIMENTAL PROPERTIES.

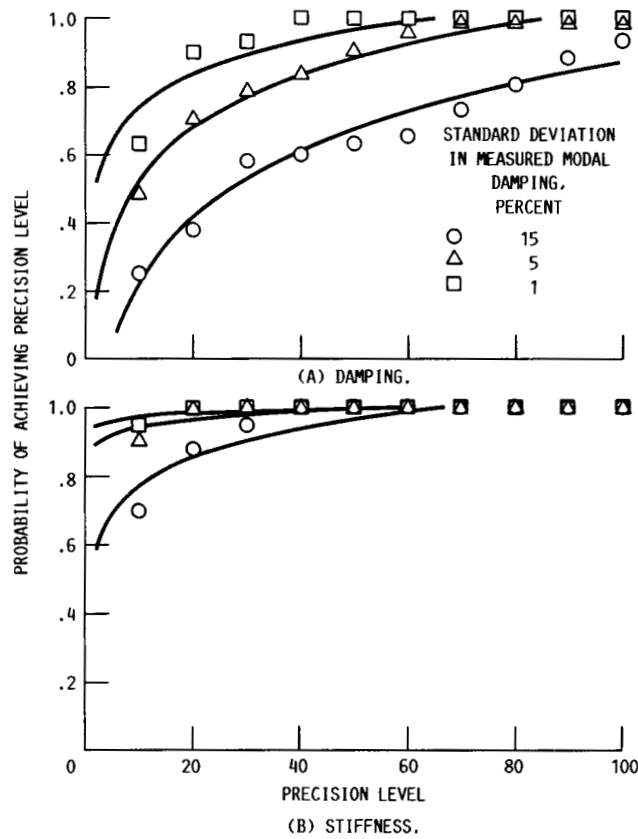


FIGURE 7. - PRECISION LEVEL, PERCENT DIFFERENCE BETWEEN IDENTIFIED AND ACTUAL PROPERTIES. ( $n = 4$ ,  $m = 1.2$ , STANDARD DEVIATION IN MEASURED FREQUENCIES = 1%).

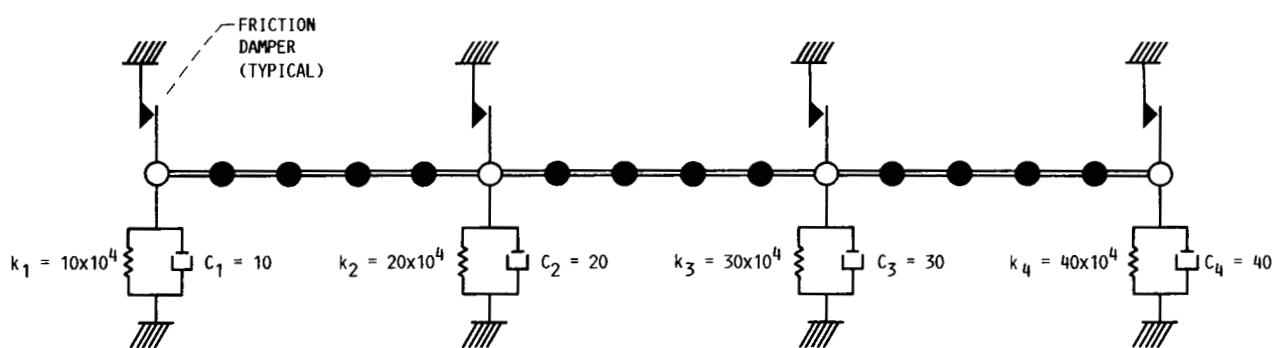


FIGURE 8. - THREE COMPONENT SYSTEM WITH FRICTION DAMPING.

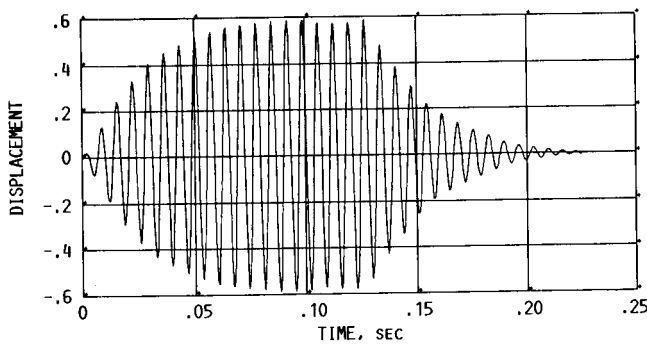


FIGURE 9. - TRANSIENT RESPONSE FOR MODE 3 AND FRICTION FORCE RATIO,  $r = 0.02$ .

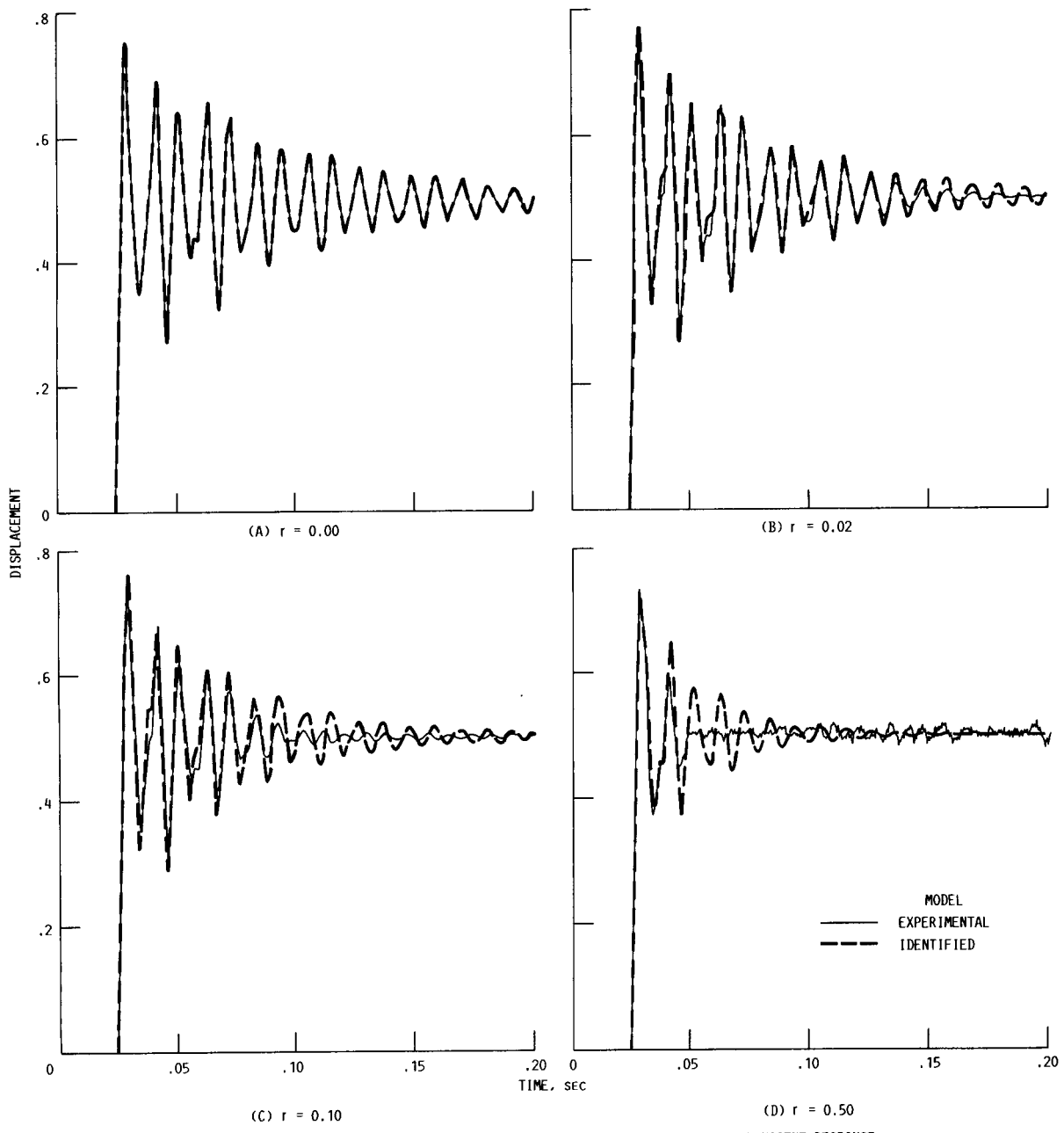


FIGURE 10. - COMPARISON BETWEEN EXPERIMENTAL AND IDENTIFIED MODELS' TRANSIENT RESPONSE.

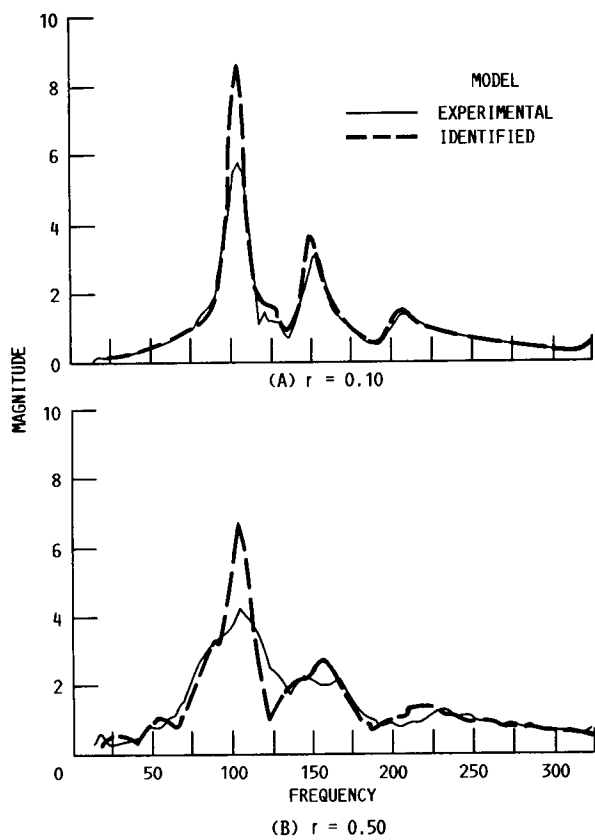


FIGURE 11. - FOURIER TRANSFORM OF DISPLACEMENT RESPONSE.

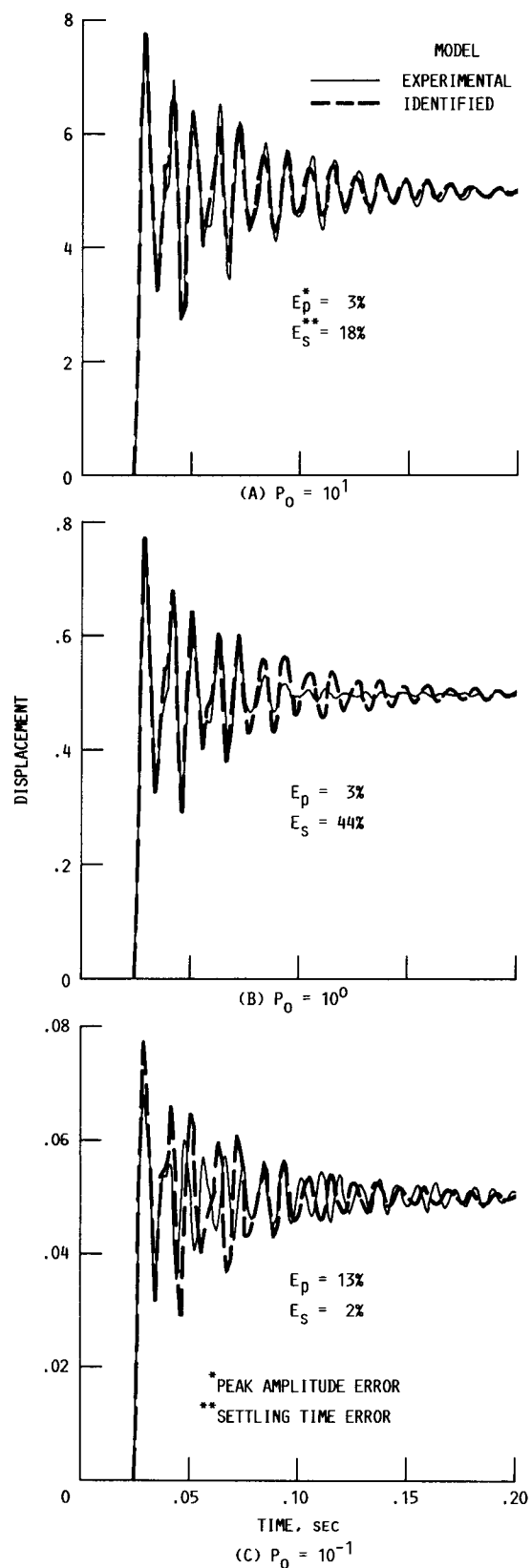


FIGURE 12. - STEP INPUT MAGNITUDE EFFECTS ON AMPLITUDE AND SETTLING TIME ERRORS,  $r = 0.10$ .



National Aeronautics and  
Space Administration

## Report Documentation Page

1. Report No.  NASA TM-100801	2. Government Accession No.	3. Recipient's Catalog No.	
4. Title and Subtitle  Characterization of Damped Structural Connections for Multi-Component Systems		5. Report Date  March 1988	
		6. Performing Organization Code	
7. Author(s)  Charles Lawrence and Arthur A. Huckelbridge		8. Performing Organization Report No.  E-3980	
		10. Work Unit No.  505-63-1B	
9. Performing Organization Name and Address  National Aeronautics and Space Administration Lewis Research Center Cleveland, Ohio 44135-3191		11. Contract or Grant No.	
		13. Type of Report and Period Covered  Technical Memorandum	
12. Sponsoring Agency Name and Address  National Aeronautics and Space Administration Washington, D.C. 20546-0001		14. Sponsoring Agency Code	
15. Supplementary Notes  Charles Lawrence, NASA Lewis Research Center; Arthur A. Huckelbridge, Case Western Reserve University, Cleveland, Ohio 44106.			
16. Abstract  The inability to model connections adequately has historically limited the ability to predict overall system dynamic response. Connections between structural components are often mechanically complex and difficult to accurately model analytically. Improved analytical models for connections are needed to improve system dynamic predictions. This study explores combining Component Mode Synthesis methods for coupling structural components with Parameter Identification procedures for improving the analytical modeling of the connections. Improvements in the connection stiffness and damping properties are computed in terms of physical parameters so the physical characteristics of the connections can be better understood, in addition to providing improved input for the system model.			
17. Key Words (Suggested by Author(s))  Parameter identification Structural connections		18. Distribution Statement  Unclassified - Unlimited Subject Category 39	
19. Security Classif. (of this report)  Unclassified	20. Security Classif. (of this page)  Unclassified	21. No of pages  18	22. Price*  A02 .